EUROPEAN ORGANIZATION FOR NUCLEAR RESEARCH

Letter of Intent to the ISOLDE and Neutron Time-of-Flight Committee

Seniority versus alpha-clustering in the Po isotopes.

Jan. 2022

G. Georgiev[1], G. Rainovski[2], A.N. Andreyev[3], N.N. Arsenyev[4], A. Astier[1], D.L. Balabanski[5], A. Barzakh[6], A. Blazhev[7], J.G. Correia[8], C. Costache[9], J. Cubiss[3], L. Fraile[10], S. Franchoo[1], K.A. Gladnishki[2], H. Haas[11], R. Heinke[12], K. Johnston[12], J. Jolie[7], D. Kocheva[2], A. Kusoglu[13], R. Lica[12], J. Ljungvall[1], N. Marginean[9], C. Mihai[9], R.E. Mihai[9], H. Naïdja[14], Ch. Page[3], S. Pascu[9], J. Röder[11], S. Röthe[12], T. Shneidman[4], C. Sotty[9], M. Stoyanova[2], K. Stoychev[1], A.E. Stuchbery[15], A. Turturica[9], N. Warr[7], Z. Yue[3]

1. IJCLab/IN2P3/CNRS, University Paris-Saclay, Orsay, France
2. Faculty of Physics, St. Kliment Ohridski University of Sofia, 1164 Sofia, Bulgaria
3. University of York, York, UK
4. Joint Institute for Nuclear Research, Dubna 141980, Russia
5. ELI-NP, NIPNE, Bucharest, Romania
6. PNPI, Gatchina, Russia
7. IKP, University of Cologne, Cologne, Germany
8. C2TN, Instituto Superior Técnico, Universidade de Lisboa, Portugal
9. "Horia Hulubei" National Institute of Physics and Nuclear Engineering, Bucharest, Romania
10. Complutense University, Madrid, Spain
11. Dept. of Physics and CICECO, University of Aveiro, Portugal
12. ISOLDE, CERN, Switzerland
13. Department of Physics, Faculty of Science, Istanbul University, Vezneciler/Fatih, Istanbul, Turkey
14. Université Constantine 1, LPMS, Constantine 25000, Algeria
15. The Australian National University, Canberra, Australia

Spokesperson(s): G. Georgiev (georgi.georgiev@ijclab.in2p3.fr)
and G. Rainovski (rig@phys.uni-sofia.bg)

Local contact: K. Johnston (karl.johnston@cern.ch)

CERN-INTC-2022-003 / INTC-I-239
04/01/2022

Abstract

The region of the nuclear chart North-East of ^{208}Pb is usually discussed in terms of an interplay between α-cluster and seniority structures. Within the shell model description, the Po isotopes, with two protons above the Z=82 shell closure, should represent a very simple case of an inert core plus very few valence nucleons. However, there are also indications that both higher-excited and low-lying yrast states could have considerable α-cluster components. Nuclear moment observables, with their sensitivity to specific components of the nuclear wave function, should be able to distinguish between these two competing approaches. However, there are several experimental difficulties for the studies of those isomers, e.g. high isobaric contamination and their very short lifetimes.

In the present Letter of Intent, we require two developments, namely: i) test of the applicability of the TDPAC technique for very short-lived isomeric states (~1 ns); and ii) test of the isobaric contamination of the bismuth isotopes using a LIST ion source. Those two developments should allow the identification of the optimal experimental conditions for performing nuclear moment studies of short-lived isomeric states in the Po isotopes in the vicinity of ^{208}Pb.

Requested shifts: 4 shifts, (split into 2 runs)

Physics motivation

The Po isotopes, with two protons above the Z=82 shell closure, represent a very interesting testing ground for the nuclear shell model. In the extreme case of ^{210}Po (^{208}Pb + 2 protons), it could be expected that its low-energy structure is dominated by excitations of those two protons, giving rise to a seniority-like pattern, which is observed as decreasing energy splitting between adjacent states with increasing spin (see Fig. 1 for ^{210}Po). Indeed, the first 4 excited states, 2^+, 4^+, 6^+ and 8^+ are indicated as belonging to the $(\pi h_{9/2})^2$ multiplet [SHA14]. The transition probabilities for those states are experimentally known. They are very well reproduced within shell model calculations (see e.g. Ref. [COR99, CAU03]) for the three higher-lying states (4^+, 6^+ and 8^+). However, there is a factor of 6 discrepancy between the theoretical calculations and the experimental B(E2, $2^+ \rightarrow 0^+$) value. A recent experimental study [KOC17a] reported a considerably different transition probability, reducing the discrepancy to a "*mere factor of 2*" with the shell model description. This already indicates that the seniority scheme may not be fully valid for the low-spin states in ^{210}Po.

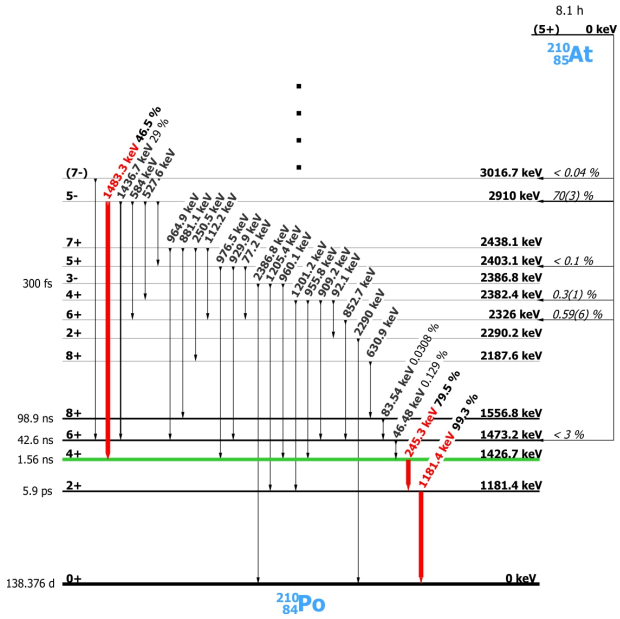

Fig. 1. Partial level scheme of ^{210}Po, populated in the beta-decay of ^{210}At. The γ-ray transitions indicated in red could be used for a TDPAC measurement of the g factor of the 4^+ state.

It is well known that transition probabilities and magnetic moment observables probe different components of the nuclear wave function. Transition probabilities can provide information on quadrupole correlations and collective degrees of freedom, while the magnetic dipole moments (μ = g*I, where the g is the g factor and I is the spin of the nuclear state) are most sensitive towards spin-flip admixtures. Therefore, these two experimental observables are complementary and indispensable for the detailed understanding of the structure of specific states. Within the seniority scheme the valence nucleons occupy a single-*j* orbital and, according to the g-factor additivity

relation, the g factor of the different $(j_n)^J$ states should be identical, independently of their spins. The g factors of the 6^+ and the 8^+ states in ^{210}Po have been measured and their values, $g(6^+) = 0.913(8)$ and $g(8^+) = 0.919(6)$ [HAU76], could be considered identical within the experimental uncertainties. At present, there are no experimental data for the g factors of the lower-spin states. Considering that the transition probability of the 2^+ state in ^{210}Po indicates a clear departure from the seniority scheme it is important to measure the g factor of the 4^+ and verify whether it deviates from the additivity relation. Its half-life, $t_{1/2}$ (4^+) = 1.56(6) ns, (see Fig.1) may allow measuring its g factor. For this purpose, one could use the Time Dependent Perturbed Angular Correlation (TDPAC) technique, which is usually applied for lifetimes in the range of ~10 ns to a few microseconds. Therefore, one of our requests in the present LoI is to perform a test measurement on the 4^+ state of ^{210}Po. Provided successful, this would pave the way to a number of short-lived isomers e.g. in ^{212}Po (6^+) or the 8^+ isomers in ^{214}Po, ^{216}Po, ^{218}Po [ANDLI].

Another key nucleus in the proposed study is ^{212}Po. It has two valence protons and two valence neutrons with respect to the doubly magic ^{208}Pb core. Similarly, to ^{210}Po, the low-lying level structure of ^{212}Po is expected to follow closely the seniority scheme with an yrast sequence of $2^+ - 4^+ - 6^+ - 8^+$ states. A high-spin isomer (18^+), having half-life much longer than the ground state ($t_{1/2}(18^+) = 45$ s; $t_{1/2}(0^+) = 294$ ns), has been observed in early studies [PER62]. The latest reported β-decay study of ^{212}Bi $\rightarrow$ ^{212}Po [LEM80] dates back from the early 80's. The $t_{1/2}$ = 25 min (9^-) isomer in ^{212}Bi populated the yrast sequence up to the 8^+ state in ^{212}Po. Important α-branching from those states have been reported in that study.

The early efforts to understand the yrast sequence of ^{212}Po in the framework of shell models were based on limited experimental data, namely the energy of the states, the lifetimes of the 8^+ and the 6^+ states, the large α-decay width of the ground state, and the large α-decay branches of the excited states. These studies have emphasized the importance of configuration mixing [TON79, JAN82] but also have revealed a discordance that, while the energies of the yrast states of ^{212}Po are well reproduced [POL87, STR79, WAR91a], the known transition strengths and the large α-decay width of the ground state are strongly underestimated [POL87, TON79, WAR91a, DOD84]. The latter has been amended by strongly mixing shell-model and α-cluster configurations [VAR92]. By including α-clustering in the structure of the low-lying yrast states of ^{212}Po the B(E2) transition strengths for the 8^+ and the 6^+ states have also been fairly well reproduced [HOY94, BUC96]. This led to the deduction that these states of ^{212}Po contain a large fraction of α-cluster components [HOY94, BUC96, BUC94, OHK95].

An extensive level scheme of the higher-energy structure of ^{212}Po has been obtained from γ–γ coincidence experiments by Poletti *et al.* [POL87] and later on by Astier *et al.* [AST10]. They found strong experimental evidence for the presence of large α-cluster components in the wave functions of states of non-natural parity at excitation energies above 1.7 MeV. However, a very recent study by Fernandez *et al.* [FER21] questions the previous interpretations and claims that those states could very well be interpreted within the shell model calculations without the need to include α-cluster components.

Some recent experiments on the lifetimes of the 2^+, 4^+, and 6^+ states of ^{212}Po [KOC17, TRE21, KAR21] have supplied the full set of transition strengths between the low-lying yrast states of ^{212}Po. It also has been demonstrated [KOC17] that single-*j* shell model calculations describe the available experimental data for the low-lying states of ^{212}Po with the exception of the $2^+_1 \rightarrow 0^+_1$ transition, for which the calculated strength is significantly overestimated. It has been argued that this problem is caused by additional contributions in the wave function of the ground state which could not be described by the shell model [WAR91, KAR19].

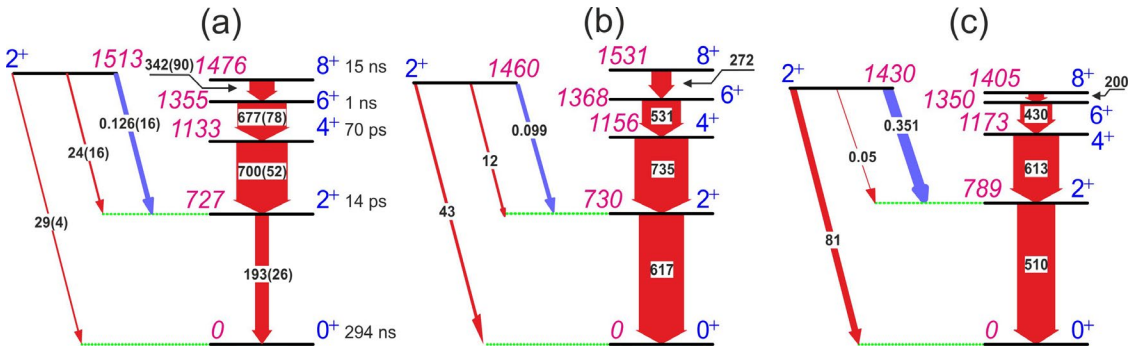

Fig. 2. Comparison of experimental low-lying positive-parity excited states of ^{212}Po (a) with the results from the shell model calculations with the H208 [NAI21] (b) and the KHPE interaction (c). The experimental data are from Ref. [KAR21]. The widths of the arrows are proportional to the E2 (red) transition strengths in e^2fm^4 and the M1 (blue) transition strengths in μ_N^2. The strengths are also presented by the numbers on the arrows.

It has to be noted that even the full set of transition strengths between the low-lying yrast states of ^{212}Po is not sufficient to provide a clear answer to the question whether they contain significant α-cluster components as can be seen from the interpretations in Ref. [TRE21, KAR21]. In Ref. [KAR21] a pure shell model approach, based on the newly developed interaction H208 [NAI21], has been adopted. The comparison between the experimental results and the theoretical calculations is shown in Figures 2 and 3. Effective charges of (e_π, e_ν) = (1.5e, 0.85e) have been used for the calculated B(E2) transition strengths. Altogether, with the exception of the $2^+_1 \rightarrow 0^+_1$ transition, the shell-model transition rates follow the behavior of experimental ones, in particular their decrease toward the 8^+_1 state (see Fig. 3). More importantly, the calculations correctly reproduce the newly determined B(E2;$4^+_1 \rightarrow 2^+_1$) value [TRE21, KAR21] indicating the shell model correctly describes the wave function of the 2^+_1 state. However, the known problem for the B(E2; $2^+_1 \rightarrow 0^+_1$) transition rate still persists, with the calculation overestimating the experimental value more than three times (see Fig. 2). These observations have led to the interpretation that the low-lying excited states of ^{212}Po can be well described by the shell model without the need of α-clustering and only the wave function of the ground state of ^{212}Po has additional contributions, outside the shell model. Most probably these contributions might be associated with α-clustering which could intuitively be expected as the ground state has a very large α-decay width.

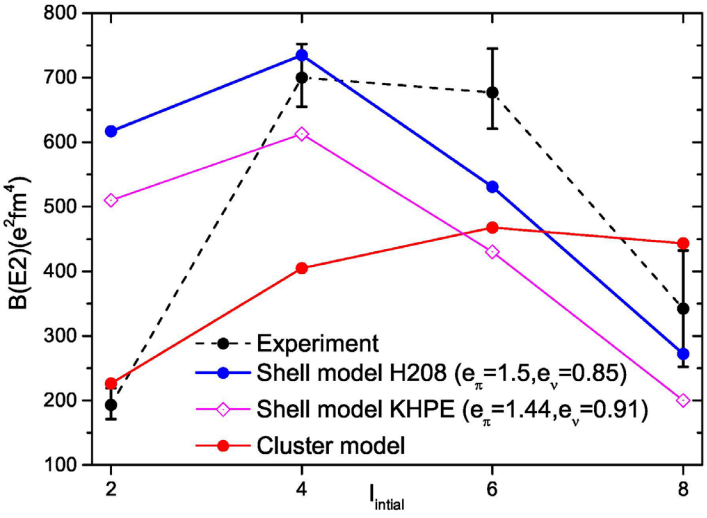

Fig. 3. B(E2) values of the transitions between the yrast states of ^{212}Po as function of the initial angular momentum. The experimental data is given in black [KAR21], the results from theoretical calculations are using the H208 interaction [NAI21] (in blue), the KHPE interaction (in magenta), and from the cluster model [TRE21] (in red). The lines are drawn to guide the eyes.

In addition to the H208 interaction, the modified Kuo-Herling interaction [WAR91] (also known as KHPE) is also widely used for shell model calculations in the region. The KHPE results are very similar to those of the H208 interaction (see Figs. 2 and 3). Although using slightly different effective charges (see Fig. 3) the overall trend is very similar to the one of the H208 interaction.

An α-cluster model interpretation has been chosen in Ref. [TRE21]. It describes adequately the overall experimental trend and provides much better agreement for the transition probability of the 2^+ state. Therefore, the authors conclude that α-cluster components play an important role in the structures of these states.

As it becomes obvious, the transition probabilities themselves, even considering the full data set, are not sufficient to clearly distinguish between the shell-model and the α-cluster description of the low-lying yrast states in ^{212}Po. Therefore, we are turning towards the magnetic moment observable, for which, unfortunately, there are no experimental data up to now. The theoretical calculations of the different models vary widely both in the predicted nuclear moments and in the used effective g factors. For example the shell model calculations using the H208 interaction utilize effective g factors for protons ($g^s_{eff} = \mathbf{0.97}*g^s_{free}$; $g^l_{eff} = \mathbf{0.85}$) and neutrons ($g^s_{eff} = \mathbf{0.27}*g^s_{free}$; $g^l_{eff} = \mathbf{0.004}$) [NAI21] in order to predict the g factors of the 8^+ and the 6^+ states as $g(8^+) = 0.072$ and $g(6^+) = 0.044$. Within the KHPE shell model calculations, the effective g factors, as recommended by Arima *et al.* [ARI87], are ($g^s_{eff} = \mathbf{0.63}*g^s_{free}$; $g^l_{eff} = \mathbf{1.13}$) for protons and ($g^s_{eff} = \mathbf{0.53}*g^s_{free}$; $g^l_{eff} = \mathbf{-0.08}$) for neutrons. The calculated g factors of the 8^+ and 6^+ states are, respectively, $g(8^+) = -0.177$ and $g(6^+) = -0.135$. These are considerably different from those obtained by the H208 interaction not only in absolute value but in their signs as well. The α-cluster model predictions for the g factors of the *pure cluster component* of the 8^+ and 6^+ are $g(8^+) = 0.064$ and $g(6^+) = 0.075$ [SHNEI]. The actual g factors of those states will depend on the admixture between the shell-model and the α-cluster components. At this point, it becomes clear that an experimental determination of the g factors of the 6^+ and 8^+ states can provide decisive information both on their shell-model descriptions and on the importance of the α-cluster component in their structure. This is well appreciated in the final conclusions of Ref. [TRE21] calling for experimental information on the static electromagnetic moments as a necessary element to prove their conjecture for the role of the α-cluster components.

It is worth mentioning that the experimental interest towards the structure of the neutron-rich Po isotopes at ISOLDE has been quite high. Fast-timing studies in ^{214}Po, ^{216}Po and ^{218}Po, following the beta-decay of the respective bismuth isotopes (IS650) have provided lifetimes for the 2^+ - 4^+ - 6^+ - 8^+ sequence in those. The lifetimes of the 8^+ states are slightly shorter than 1 ns [ANDLI], which comes close to the limit of applicability of the TDPAC technique. Provided that the measurement of the 6^+ state in ^{212}Po proves successful, this might pave the way towards the studies of the more exotic nuclei.

Experimental approach

The experimental technique to be used for the nuclear moment studies of the short-lived isomeric states in the Po isotopes is the Time Dependent Perturbed Angular Correlations (TDPAC). It is based on the perturbation of the angular correlation between two gamma rays, one of which is populating and the second one – depopulating the isomeric state of interest. Populating the states above the isomer of interest in beta-decay provides low-background experimental conditions.

The TDPAC technique is standardly applicable on isomeric states with lifetimes in the range of "a few nanoseconds" up to a few microseconds. The short-lifetime limit of the technique is determined by two factors: i) obtaining a sufficiently strong magnetic field, which would allow for a complete spin rotation within the nuclear lifetime; and ii) the time resolution of the gamma-ray detectors, which should be better than the half-period of the oscillations. An important experimental advantage in the case of the Po isotopes is the very strong hyperfine field observed after their implantation in ferromagnetic materials. For example, the hyperfine fields of Po in Fe and Ni are, respectively, 238

T and 66 T (at "0 K"). This would allow the observation of a full period of the nuclear-spin rotation within 3 ns for g factors down to 0.1, when implanted in Fe. Considering the half-lives of the 4^+ state in ^{210}Po ($t_{1/2}$ = 1.56 ns) and the 6^+ state in ^{212}Po ($t_{1/2}$ = 1ns) they should be within reach. The use of $LaBr_3$(Ce) detectors should provide sufficient time resolution for observing the oscillation patterns even for periods shorter than 1 ns. The combination between implantation in Fe, for the short-lived, small-g-factor states, and in Ni, for the longer-lived states, would provide suitable experimental conditions for g-factor measurement of isomeric states with half-lives in the range 1 to 20 ns and g-factor range 0.1 – 0.9. A calibration measurement, using the 6^+($t_{1/2}$ = 4 ns) isomeric state in ^{208}Po, which has a known g factor, would allow to determine the effective hyperfine fields in Ni and Fe at room temperature.

The long lifetimes of ^{210}At ($t_{1/2}$ = 8h) and ^{208}At ($t_{1/2}$ = 98 min) will allow performing the ^{210}Po and ^{208}Po measurements in an off-line mode with an already existing setup. For the ^{212}Po measurement ($t_{1/2}$(^{212}Bi) = 25 min), due to the shorter half-life, an on-line approach will be used. An on-line TDPAC setup is presently being constructed for the IS673 experiment and will be available in the summer of 2022.

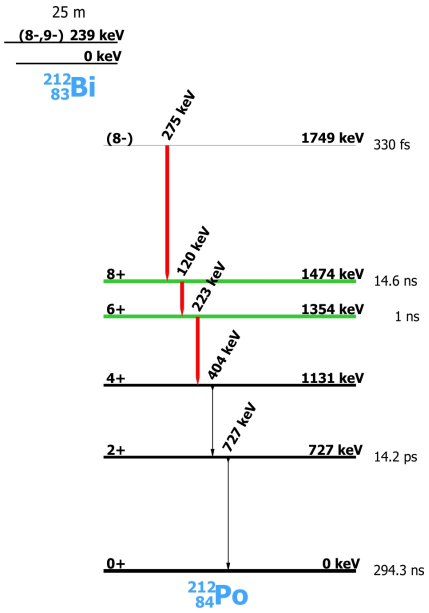

Fig. 4. Partial level scheme of ^{212}Po, populated in the beta-decay of ^{212m}Bi

Population of the states of interest

The 8^+ states in ^{212}Po, and in the higher-mass ^{214,216,218}Po isotopes, could be populated in the β-decay of the respective Bi isotopes (their higher-spin isomers). An example for ^{212}Po is given in Fig. 4. However, it is not trivial to obtain sufficiently pure beams of those Bi isotopes using an UC_x target at ISOLDE (see Fig. 5). Francium (an alkali metal) is a notorious contaminant in this mass region, which usually comes (from surface ionization) at rates several orders of magnitude higher than the isotopes of interest. A way to overcome this problem has been found for some specific cases (see e.g. experiment IS650). For example, the lifetimes of the francium isotopes with masses between 214 and 218 are extremely short (less than 5 ms) thus they hardly get released from the target.

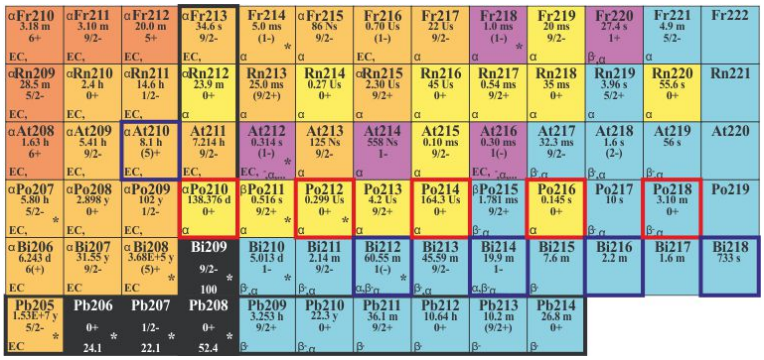

Fig. 5. Part of the nuclide chart North of lead isotopes.

However, for masses below 214, and above 219, the lifetimes of the francium and the bismuth isotopes are comparable and this technique is inapplicable. Therefore, in the present LoI we request that a different approach is applied, namely the use of a LIST ion source. It has already been tested in the lower mass regions and has shown levels of suppression of the surface contaminants of several orders of magnitude. However, there are also some indications that in the heavy mass region, for nuclei populated thorough alpha decay, the suppression efficiency of the LIST ion source might be considerably reduced. ***Therefore, comes our request to test the LIST ion source for the production of ^{212}Bi, ^{219}Bi and ^{220}Bi.*** For this purpose, the IDS could be considered as a versatile setup that would allow performing the yield check especially for the low-intensity1 cases.

Contrary to the neutron-rich Po isotopes, populated in the β-decay of the respective bismuth isotopes, the isomeric state of ^{210}Po can be populated in the β-decay of ^{210}At (see Figures 1 and 5). The ^{210}At isotope can be produced using a lead-bismuth target, in which the francium isotopes cannot be populated. The yield of ^{210}At (from a Pb/Bi target) has already been measured as $7x10^7$ pps/μC. Therefore, this approach would allow obtaining a very pure beam of ^{210}At with sufficient intensity. ***Here comes our second request in this LoI – to use a Pb/Bi target for testing the TDPAC technique*** for very short-lived isomers (~1ns and lower). Provided successful, this should allow submitting a full-fledged proposal aiming at nuclear moment studies of the 6^+ and the 8^+ isomers in ^{212}Po as well as the newly observed isomers in ^{214}Po, ^{216}Po and ^{218}Po [ANDLI].

Summary of requested shifts:

In summary we request:

- **1 shift** for ^{210}At and **1 shift** for ^{208}At, both produced using Pb/Bi target;
- **2 shifts** for LIST ion source test using UC_x target.

References:

[ANDLI] A.N. Andreyev and R. Lica, private communication and IS650 proposal https://cds.cern.ch/record/2288193/files/INTC-P-529.pdf

[ARI87] A. Arima, K. Shimizu,W. Bentz, and H. Hyuga, in Advances in Nuclear Physics, edited by J. W. Negele and E. Vogt (Plenum, New York, 1987), Vol. 18, p. 1.

[AST10] A. Astier, *et al.*, Phys. Rev. Lett. **104**, 042701 (2010); A. Astier, *et al.*, Eur. Phys. J. **A 46**, 165 (2010).

[BUC94] B. Buck, A.C. Merchant, S.M. Perez, Phys. Rev. Lett. **72**, 1326 (1994).

[BUC96] B. Buck, J.C. Johnston, A.C. Merchant, S.M. Perez, Phys. Rev. **C 53**, 2841 (1996)

[CAU03] E. Caurier, *et al.*, Phys. Rev. **C 67**, 054310 (2003).

[COR99] L. Coraggio, *et al.*, Phys. Rev. **C 60**, 064306 (1999).

[DEL12] D.S. Delion, *et al.*, Phys. Rev. **C 85**, 064306 (2012).

[DOD84] G. Dodig-Crnkovic, F. A. Janouch, and R. J. Liotta, Phys. Lett. **B 139**, 143 (1984).

[HAU76] O. Häusser *et al.*, Nucl. Phys. A273, 253 (1976).

[HOY94] F. Hoyler, P. Mohr, G. Staudt, Phys. Rev. **C 50**, 2631 (1994).

[JAN82] F. A. Janouch and R. J. Liotta, Phys. Rev. **C 25**, 2123 (1982).

[KAR19] V. Karayonchev *et al.*, Phys. Rev. C 99, 024326 (2019).

[KAR21] V. Karayonchev *et al.*, submitted to Phys. Rev. C (2021).

[KOC16] D. Kocheva *et al.*, Phys. Rev. **C 93**, 011303(R) (2016).

[KOC17] D. Kocheva *et al.*, Phys. Rev. **C 96**, 044305 (2017).

[KOC17a] D. Kocheva *et al.*, Eur. Phys. J. A 53, 175 (2017).

[LEM80] P. Lemmertz *et al.*, Z. Phys. **A 298**, 311 (1980).

[NAI21] Houda Naïdja, Phys. Rev. **C 103**, 054303 (2021).

[FER21] A. Fernández *et al.*, Phys. Rev. C 104, 054316 (2021).

[OHK95] S. Ohkubo, Phys. Rev. Lett. **74**, 2176 (1995).

[PER62] I. Perlman, F. Asaro, A. Giorso, A. Larsh, R. Latimer, Phys. Rev. **127**, 197 (1962).

[POL87] A.R. Poletti *et al.*, Nucl. Phys. **A 473**, 595 (1987).

[SHA14] M. Shamsuzzoha Basunia, Nucl. Data Sheets **121**, 561 (2014).

[SHNEI] T.M. Shneidman, private communication.

[STR79] D. Strottman, Phys. Rev. **C 20**, 1150 (1979).

[TON79] I. Tonozuka and A. Arima, Nucl. Phys. **A 323**, 45 (1979).

[TRE21] M. von Tresckow *et al.*, Phys. Lett. **B 821**, 136624 (2021).

[VAR92] K. Varga, R. G. Lovas, and R. J. Liotta, Phys. Rev. Lett. **69**, 37 (1992).

[WAR91] E.K. Warburton and B. A. Brown, Phys. Rev. **C 43**, 602 (1991).

[WAR91a] E.K. Warburton, Phys. Rev. **C 44**, 261 (1991).

Appendix

DESCRIPTION OF THE PROPOSED EXPERIMENT

The experimental setup comprises: *(name the fixed-ISOLDE installations, as well as flexible elements of the experiment)*

Part of the Choose an item.	Availability	Design and manufacturing
On-line PAC	☒ In preparation for IS673	☒ To be used without any modification
IDS	☒ Existing	☒ To be used without any modification

HAZARDS GENERATED BY THE EXPERIMENT

(if using fixed installation) Hazards named in the document relevant for the fixed [COLLAPS, CRIS, ISOLTRAP, MINIBALL + only CD, MINIBALL + T-REX, NICOLE, SSP-GLM chamber, SSP-GHM chamber, or WITCH] installation.

Additional hazards:

Hazards			
	[Part 1 of the experiment/equipment]	*[Part 2 of the experiment/equipment]*	*[Part 3 of the experiment/equipment]*
Thermodynamic and fluidic			
Pressure	[pressure][Bar], [volume][l]		
Vacuum			
Temperature	[temperature] [K]		
Heat transfer			
Thermal properties of materials			
Cryogenic fluid	[fluid], [pressure][Bar], [volume][l]		
Electrical and electromagnetic			
Electricity	[voltage] [V], [current][A]		
Static electricity			
Magnetic field	[magnetic field] [T]		
Batteries	☐		
Capacitors	☐		
Ionizing radiation			
Target material	[material]		
Beam particle type (e, p, ions, etc)			
Beam intensity			
Beam energy			
Cooling liquids	[liquid]		
Gases	[gas]		
Calibration sources:	☐		
• Open source	☐		
• Sealed source	☐ [ISO standard]		
• Isotope			
• Activity			
Use of activated material:			

• Description	☐		
• Dose rate on contact and in 10 cm distance	[dose][mSV]		
• Isotope			
• Activity			
Non-ionizing radiation			
Laser			
UV light			
Microwaves (300MHz-30 GHz)			
Radiofrequency (1-300MHz)			
Chemical			
Toxic	[chemical agent], [quantity]		
Harmful	[chemical agent], [quantity]		
CMR (carcinogens, mutagens and substances toxic to reproduction)	[chemical agent], [quantity]		
Corrosive	[chemical agent], [quantity]		
Irritant	[chemical agent], [quantity]		
Flammable	[chemical agent], [quantity]		
Oxidizing	[chemical agent], [quantity]		
Explosiveness	[chemical agent], [quantity]		
Asphyxiant	[chemical agent], [quantity]		
Dangerous for the environment	[chemical agent], [quantity]		
Mechanical			
Physical impact or mechanical energy (moving parts)	[location]		
Mechanical properties (Sharp, rough, slippery)	[location]		
Vibration	[location]		
Vehicles and Means of Transport	[location]		
Noise			
Frequency	[frequency],[Hz]		
Intensity			
Physical			
Confined spaces	[location]		
High workplaces	[location]		
Access to high workplaces	[location]		
Obstructions in passageways	[location]		
Manual handling	[location]		
Poor ergonomics	[location]		

3.1 Hazard identification

3.2 Average electrical power requirements (excluding fixed ISOLDE-installation mentioned above): *(make a rough estimate of the total power consumption of the additional equipment used in the experiment)*